Dalton Transactions

Accepted Manuscript

Volume 45 | Number 1 | 7 January 2016 | Pages 1–398

Dalton Transactions

An international journal of inorganic chemistry
www.rsc.org/dalton

ISSN 1477-9226

PAPER
Joseph T. Hupp, Omar K. Farha et al.
Efficient extraction of sulfate from water using a Zr-metal–organic framework

175 YEARS

This is an Accepted Manuscript, which has been through the Royal Society of Chemistry peer review process and has been accepted for publication.

Accepted Manuscripts are published online shortly after acceptance, before technical editing, formatting and proof reading. Using this free service, authors can make their results available to the community, in citable form, before we publish the edited article. We will replace this Accepted Manuscript with the edited and formatted Advance Article as soon as it is available.

You can find more information about Accepted Manuscripts in the author guidelines.

ROYAL SOCIETY OF CHEMISTRY

rsc.li/dalton

Journal Name

ARTICLE

Rapid Self-Healing and Anion Selectivity in Metallosupramolecular Gels Assisted by Fluorine-Fluorine Interactions

Leticia Arnedo-Sánchez,[a] Nonappa,[b] Sandip Bhowmik,[a] Sami Hietala,[c] Rakesh Puttreddy,[a] Manu Lahtinen,[a] Luisa De Cola[d] and Kari Rissanen[a*]

Simple ML_2 [M= Fe(II), Co(II), Ni(II)] complexes obtained from a perfluoroalkylamide derivative of 4-aminophenyl-2,2′,6,2′-terpyridine spontaneously, yet anion selectively, self-assemble into gels, which manifest an unpresetended rapid gel strength recovery, viz. self-healing, and thermal rearrangement in aqueous dimethyl sulfoxide. The key factor for the gelation and the rheological properties emerge from the fluorine - fluorine interactions between the perfluorinated chains, as the corresponding hydrocarbon derivative did not from metallogels. The perfluoro-terpyridine ligand alone formed single crystals, while its Fe(II), Co(II) or Ni(II) complexes underwent rapid gelation leading to highly entangled fibrillar networks visualized by electron microscopy. The thermodynamic parameters of gelation based on variable temperature NMR on ^{1}H and ^{19}F resonances showed that gelation was enthalpically favourable and entropically disfavoured. The step strain rheological experiments revealed that the gels undergo rapid self-healing and the morphological features, thermal stability and mechanical properties were found to depend on the nature of the metal ion.

Introduction

Metallosupramolecular self-assembly has continued to gain a new dimension due to its ability to control the shape and size of molecular, as well as, supramolecular superstructures.[1-5] Examples include self-assembly into cages,[6] cubes,[7] spheres,[8] grids,[9] helicates,[10] and metal organic frameworks.[11] In addition, the above examples also provide dynamic control for host-guest chemistry,[12] size-selective entrapment,[13] stereo-controlled chemical reactions,[14] and supramolecular polymers.[15] Recently the self-assembly process of luminescent platinum complexes has been visualized and controlled using the change in the photophysical properties of the compounds upon aggregation.[16] Supramolecular gelation on the other hand, is continuously evolving area of research with new insights and novel application potentials. Non-covalent interactions such as hydrogen bonding, π-π stacking, charge transfer interactions, and hydrophobic effects have been extensively utilized towards rational design of low molecular

mass organo- and hydrogelators with new functional properties.[17-20] Peptides,[21] carbohydrates,[22] steroids,[23] urea-derivatives,[24] and simple fatty acids,[25] have been shown to exhibit remarkable ability to self-assemble into highly entangled fibrillar networks thereby able to encapsulate and immobilize solvent molecules. While a majority of the gelators have been discovered serendipitously,[26,27] continuing efforts have been made towards rational design of gelators with tunable properties as for example thermotropic polymorphism[28] or stimuli-responsiveness[29] including anion dependent gels[30] with interesting applications in molecular sensing.[31] Recently, metal coordination induced self-assembly of small molecules leading to solvent immobilization and gelation has emerged as a fascinating area of research in the field of supramolecular gels.[32,33] In order to promote supplementary interactions and achieve supramolecular gelation, more than one non-covalent interaction is needed, thereby facilitating self-assembly at multiple length scales. As a result, additional interaction motifs such as peptide bonds, urea-linkers or steroidal units have been appended to the basic ligand units. Moreover, it has been shown that by combining the metal-ligand coordination bonds, along with additional supramolecular interactions and ligand design, the concept of subcomponent self-assembly can be used in molecular gelation.[34] Among several ligands studied for gelation, terpyridine and its derivatives were shown to be attractive candidates because of their easy synthesis and functionalization as well as for their ability to bind a diverse number of metal ions.[35,36] On the other hand, less studied interactions such as halogen bonding have been reported to control the self-assembly of a variety of motifs such as ureas[37]

[a.] Nanoscience Center, Department of Chemistry, University of Jyväskylä, P.O. Box 35, Jyväskylä, FI-40014, Finland. E-mail. kari.t.rissanen@jyu.fi
[b.] Molecular Materials Group, Department of Applied Physics, Aalto University School of Science, Puumiehenjua 2, Espoo, FI-02150, Finland.
[c.] Laboratory of Polymer Chemistry, Department of Chemistry, University of Helsinki, P.O. Box 55, FI-00014, Helsinki.
[d.] ISIS, Université de Strasbourg and CNRS UMR 7006, 8 rue Gaspard Monge, Strasbourg 67000, France

and peptides[38] leading to hydrogelation. Weak interactions including fluorine - fluorine (F⋯F) interactions, are also gaining attention in the field of contemporary supramolecular chemistry.[39-43] Previously, fluorinated solvents (fluorous)[44] and pharmaceutically important molecules[45,46] have been extensively studied. Beyond being a consequence of crystal packing, recent experimental and theoretical studies have supported the existence of F⋯F interactions and opened up new applications in supramolecular chemistry.[47,48] The fluorinated analogues of hydrocarbon compounds possess exceptional properties such as steric bulk, stiff and stable nature, simultaneous hydro- and lipophobicity, slower aggregation behaviour and lower critical gelation/aggregation concentration. These features of fluorinated counterparts offer a unique opportunity to design materials with unprecedented properties.[49] In polymer science, polyethylene glycol derivatives with terminal fluoroalkyl groups have shown to exhibit peculiar rheological properties as "*associative thickeners*".[50] Similarly, polyacrylamide with a minute amount of fluorocarbon groups have shown to associate much stronger compared to simple hydrocarbon derivatives.[51] In 1999 Hamilton *et al*. showed the gelation of partially fluorinated urea derivatives in supercritical carbon dioxide.[52] Supramolecular gels derived from fluorinated gallic acid,[37] peptides,[40] bile acids,[41] bis-urea,[42] *N*-alkylamides,[53] gemini phenoxy units[54] and biphenyl[55] have been reported in the literature. This work shows how a simple perfluoroalkylamide of 4-aminophenyl-2,2′,6,2′-terpyridine can act as a metallosupramolecular gelator. The metal-ligand coordination leads to ML$_2$ [M = Fe(II), Ni(II) and Co(II)] coordination complex and fluorine-fluorine interactions between the sidechain drive an extended lateral assembly, furnishing highly entangled fibrillar networks. The gelation is anion selective and the mechanical and thermal properties can be tuned by changing the metal cation. Further, the rheological step strain experiments show that the gels undergo a rapid self-healing[56] recovering the gel strength after release of the step strain.

Results and discussions

Synthesis and Gelation studies

The starting material 4-aminophenyl-2,2′:6′,2′′-terpyridine **2** was synthesized according to the literature procedure reported previously.[57] The gelating ligand *N*-(4-([2,2':6',2''-terpyridin]-4'-yl)phenyl)-2,2,3,3,4,4,5,5,6,6,7,7,8,8,8-penta-decafluorooctan-amide **3** was prepared by dropwise addition of pentadecafluorooctanoyl chloride **1**, to a solution of **2** in anhydrous dichloromethane and in the presence of *N,N*-diisopropylethyl amine (Fig. 1, see ESI for complete synthesis procedure and characterization). The ligand **3** upon recrystallization from chloroform formed single crystals suitable for X-ray diffraction analysis. A similar procedure was followed for the synthesis of the hydrocarbon analogue **3H** (see ESI). However, and not surprisingly, efforts to obtain single crystals remained unsuccessful. In addition, ligand **4** was prepared (Fig. 1 and ESI), which includes a partially perfluorinated chain with an ethylene moiety between the carbonyl and perfluoro groups. When a known amount of ligand **3** was dissolved in dimethyl sulfoxide (DMSO) by gentle heating, addition of a known volume of water reaching DMSO:water ratio of 5:1 (v/v), resulted in a viscous precipitate. However, the viscous material did not survive during the gelation test (test tube inversion). Interestingly, addition of 0.5 molar equivalent of aqueous metal salt (CoCl$_2$, NiCl$_2$ or FeCl$_2$) into a solution of **3** in DMSO resulted in immediate colour change followed by precipitation. The complexes upon heating led to a clear solution and upon cooling to room temperature stable coloured gels were obtained (Fig. 1, see ESI for details) showing resistance to flow upon test tube inversion. The gels underwent repeated sol-gel transition upon heating-cooling cycles. The ESI-TOF mass spectrometry on positive mode revealed the formation of ML$_2$ type complexes (see ESI), supported by NMR spectroscopy studies, which suggest the presence of a single product. In the control experiments analogous metal complexes containing ligand **3H** were found not to be gelators, thereby highlighting the importance of the perfluoroalkyl unit. The comparison of powder X-ray diffraction (PXRD) patterns of **3H** with the simulated PXRD patterns using single crystal X-ray data of **3** (Fig. S9) revealed a clear difference in the packing of the two ligands.
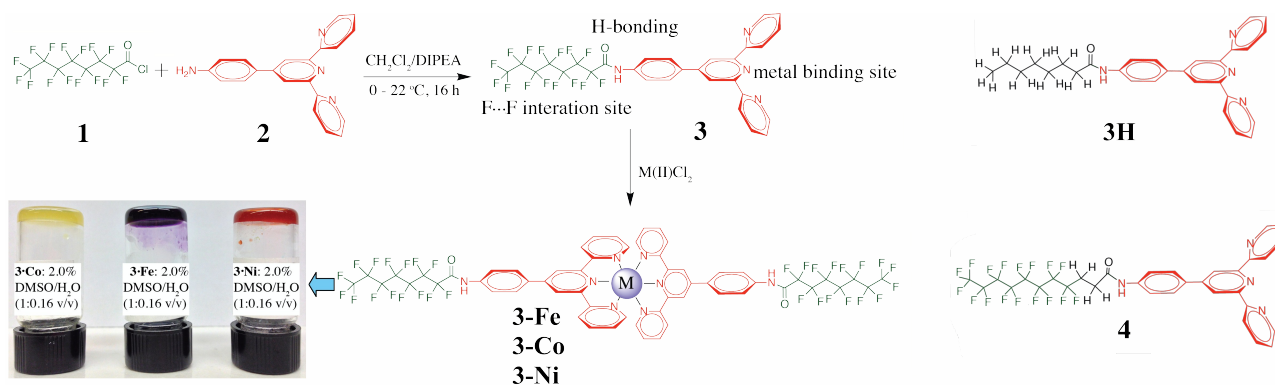

Fig. 1 Synthetic scheme of ligand **3** and its complexation with M(II)Cl$_2$ (M = Ni, Fe, Co). Photographs of **3-M** gels. Chemical structure of ligands **3H** and **4**.

Dalton Transactions

Journal Name

ARTICLE

Similarly, with the partially fluorinated side chain in **4** no gelation was observed by ligand itself or upon complexation with FeCl2. Interestingly, ligand **4** leads to weak gels upon complexation with 0.5 eq of CoCl2 (**4-Co**) or NiCl2 (**4-Ni**). The metallogels **4-M** [M = Co(II) or Ni(II)] are much less stable than their **3-M** analogues. Indeed, **4-Co** precipitates out after 6 hours and **4-Ni** crystallizes out after 36 hoursWe were pleased to observe that **4-Ni** gel evolved into good quality single crystals of [Ni**4**2]Cl2. Such an intriguing gel to crystal transition phenomenon has been previously reported and provides an excellent opportunity to investigate the potential supramolecular interactions that cause the gelation.[58] Careful examination of the crystal supports our hypothesis on supramolecular polymerisation through F···F interactions during the gelation and will be discussed in detail later. Furthermore, in order to promote polymerization and increase the strength of the supramolecular structure by the potential formation of hydrogen bonds, the perfluorinated chain was attached via amide bonds to the phenylterpyridine core. The anion seems to play also a crucial role as only chloride anions induce the gelation, whereas the use of other counter anions such as bromide, tetrafluoroborate, perchlorate, triflate or sulphate did not lead to the gel formation. More importantly, further addition of chloride ions to the non-gelling complexes turned on the gelation. This directly provides evidence that the gelation is Cl⁻ specific. The chloride salts of Fe(II), Co(II) and Ni(II) resulted in instantaneous gelation at 2.0 w/v% (mass of gelator by volume of solvent) and with a minimum gelation concentration (MGC) of < 1.0 %. The gel melting temperature (T_{gel}) and thermal stability measured using inverted test tube method showed a linear increase in the T_{gel} with increasing concentration. However, for a given concentration the gel melting trend followed the order Fe>Ni>Co (see Table 1 and ESI). The T_{gel} were sharp for **3-Fe** and **3-Co** but **3-Ni** showed a broad range of melting temperature (see Table S1 and Fig. S11).

Table 1: Gelation response of ligands **3** and **3H** towards different metal salts at 2 % DMSO : water (5:1 v/v). G = gel, S = solution. ᵃ T_{gel} of 2 % gels.

Metal Salt	Ligand **3**	Ligand **3H**
FeCl2	G(70°C)ᵃ	S
CoCl2	G(47°C)ᵃ	S
NiCl2	G(60°C)ᵃ	S
FeBr2	S	S
Fe(ClO4)2	S	S
Fe(BF4)2	S	S
FeSO4	S	S
Fe(OTf)2	S	S

Single crystal X-ray diffraction study

Single crystals of good quality for X-ray diffraction studies were obtained either in its pure form or as solvates for ligand **3** upon slow evaporation of chloroform (**3** and **3·CHCl3**), tetrahydrofuran (**3·THF**) and moist methanol (**3·CH3OH·H2O**) solutions. Systematic analysis of the X-ray structures (see Fig. 2A and B and Figs. S12-S14) revealed a slightly twisted, non-linear nature for the ligand **3** and its ability to form hydrogen bonds through the amide group. More importantly, the molecular packing also showed the extended tail to tail interactions of the perfluoroalkyl chains in addition to π-π stacking between the aromatic moieties. Therefore, in the
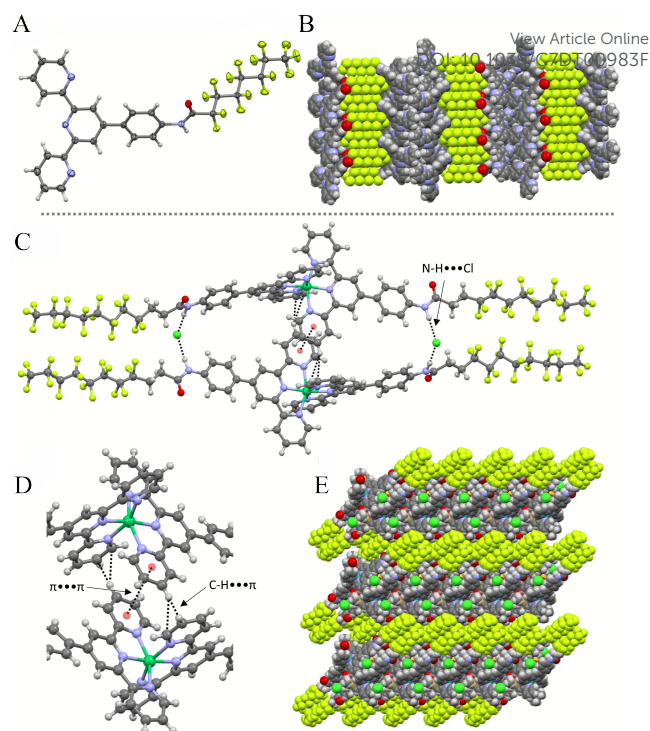

Fig. 2 (A) Crystal structure of ligand **3** with thermal displacement parameters at 50% probability level. (B) Crystal packing of ligand **3**. The lattice is constructed from F···F interactions between the perfluorinated chains and are reinforced by the N-H···O=C hydrogen bonds between adjacent molecules of **3**. (C) Crystal structure of **[Ni4₂]Cl₂** stabilized by N-H···Cl, π··π and C-H···π interactions. (D) Closer view of **[Ni4₂]Cl₂** around terpyridine core to show π··π and C-H···π interactions. (E) Crystal packing of complex **[Ni4₂]Cl₂** viewed along the *a*-axis highlighting the F···F and C-F···π interactions.

solid-state F···F interaction acts as one of the key interactions in the formation of the supramolecular structures. The packing of **3** and its solvates manifests similar F···F interactions to those shown by [Ni**4**2]Cl2 crystal (Fig. 2B and E). Additionally, the anion selectivity gelation is highly supported by the critical role that chloride anions play furnishing the hydrogen bond network as shown in Fig. 2E for [Ni**4**2]Cl2.
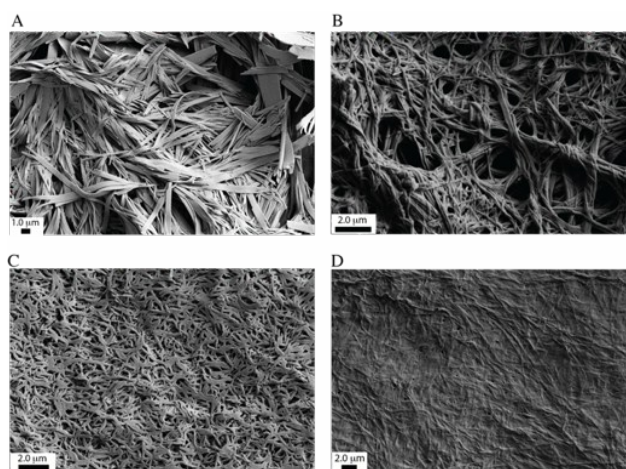
Morphology of the gels

Fig. 3 Scanning electron micrographs of dry precipitate for ligand **3** (A) and xerogels **3-Fe** (B); **3-Co** (C) and **3-Ni** (D) obtained from 2 % DMSO/H2O samples.
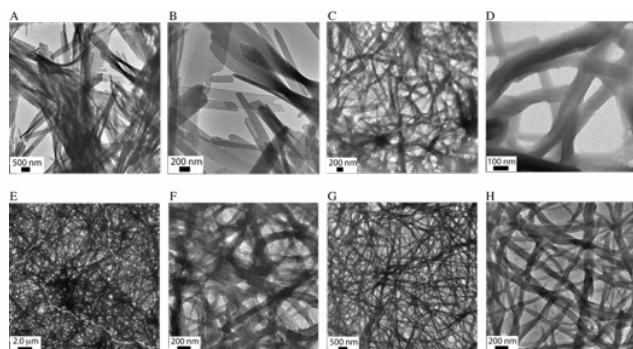
Fig. 4 Transmission electron micrographs of dry precipitate for **3** (A&B) and xerogels for **3-Fe** (C&D); **3-Co** (E&F) and **3-Ni** (G&H) obtained from 2 % DMSO/H₂O samples.

The electron microscopy of dry precipitates of ligand **3** and xerogels for metallogels **3-M** [M = Fe(II), Ni(II) or Co(II)] are shown in Fig. 3 and 4. The scanning electron microscopy (SEM) images showed that ligand **3** forms microcrystalline sheets several micrometers long and 1-2 µm wide (Fig. 3A). The absence of interconnected networks is in good agreement with the non-gelling nature of **3**. The SEM micrographs of gels derived from metal complexes showed highly entangled fibrillar networks. The diameter of the fibers range from 50 to 200 nm with indefinite length, one of the features of gels from low molecular weight gelators. The transmission electron microscopy (TEM) analysis of ligand **3** showed the presence of microcrystalline strands (Fig. 4A). The xerogels obtained from metallogels showed highly entangled fibrillar network wherein the nature and size of the fibers depend on the metal ion used in the study (Fig. 4B-D). The fiber diameter varied from 100-125 nm for **3-Fe**, 80-100 nm for **3-Co** and to 50-100 nm for **3-Ni**.

Variable temperature (VT) NMR

Solution,[59] and solid state,[60] NMR spectroscopy experiments have been extensively used to study interactions, structural changes and dynamics of gelation. However, NMR spectroscopic characterization of certain metal complexes is a challenging task due to the paramagnetic nature of these species. Therefore, out of the three metal complexes, the **3-Fe** gel was selected for NMR studies due to the diamagnetic character of the Fe(II)-terpyridine low spin complexes. In more detail, 2.0 % DMSO-d_6-D₂O gel of **3-Fe** was analysed by variable temperature (VT) ^{1}H NMR in a temperature interval from 30 to 90°C with 5°C increments. The broad signals in the gel state at room temperature turned sharper until the temperature reached 50°C. Surprisingly, at 55°C the signals turned broad again, however, further increase in temperature above 55°C led to sharp peaks. A more accurate study was performed by heating the gel sample from 40 to 70°C with 2°C increments. It was found that the transition appeared at 58°C. Further, a controlled cooling ramp (sol-gel) was performed from 85 to 30°C. Upon cooling the signals became broader until 55°C and below 55°C they turned sharper and once again continued to
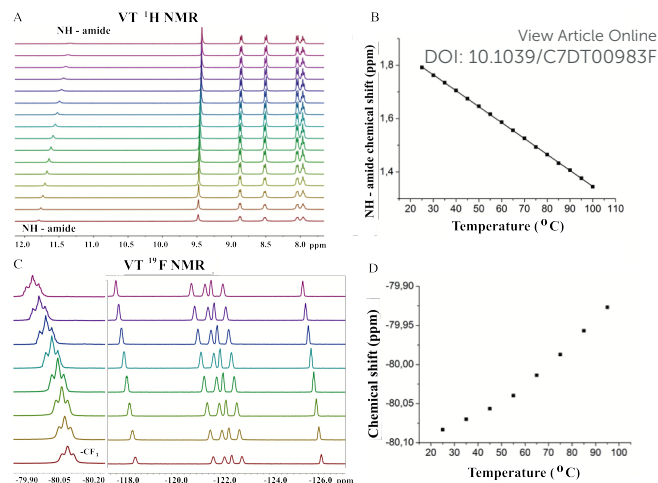

Fig. 5 Variable temperature NMR spectroscopy experiments. (A) Partial VT ^{1}H NMR spectra of 2 % DMSO-d_6 - D₂O gel of **3-Fe**. (B) Plot showing change in the chemical shift values of amide proton signal as a function of temperature. (C) VT ^{19}F NMR of 2 % DMSO-d_6 + D₂O gel of **3-Fe**. (D) Change in the chemical shift value of fluorine signals as a function of temperature.

broaden (See Fig. S17-S20). This behaviour suggests a thermally induced supramolecular rearrangement of the metal complexes. These results strongly support the hypothesis of a phase transition observed in temperature sweep rheological measurements (see next section). The VT ^{1}H NMR of the gel showed an upfield shift ($\Delta\delta$ = 0.45 ppm) for amide proton (-NH) signal from 11.79 ppm at room temperature (in gel state) to 11.34 ppm upon increasing temperature (in solution state) (Fig. 5). It can be concluded that hydrogen bonding is one of the driving forces involved in self-assembly.[56] Further, the Fourier transform infrared (FT-IR) spectroscopy studies support this observation. The FT-IR spectrum of the bulk solid **3** was compared to the xerogel of aggregates of **3** and metallogels **3-M** (M = Fe, Co, Ni). The spectrum of bulk solid **3** showed amide -NH stretching at 3323 cm⁻¹ which shifts to 3245 cm⁻¹ for the xerogels, clearly indicating the presence of hydrogen bond through the amide moieties (See Fig. S26). In order to investigate the role of fluorine a VT ^{19}F NMR experiment was performed. The ^{19}F signals underwent a progressive broadening and downfield shift upon temperature increase (Fig. 5C). Even though, the change in the chemical shift value is only 0.2 ppm, it is significant considering the strength of the F···F interaction.[40,61] Further, FT-IR was employed to investigate the influence of gelation on the C-F stretching frequency, which is usually found in the range 1000-1400 cm⁻¹. The C-F stretching frequency for bulk solid **3** exhibited two narrow peaks at 1200 and 1144 cm⁻¹. However, for the case of the metallogels **3-M** (M = Fe, Co, Ni), the former signal led to a broad band peaking at 1198 cm⁻¹ meanwhile the latter resolved into two partially merged signals at 1146 and 1130 cm⁻¹ (See Fig. S27). These results certainly indicate that the fluorine atoms play an essential role on the polymerization process,[40] in excellent agreement with the conclusions obtained by VT ^{19}F NMR. This strongly suggests the existence of robust F···F interactions in the gel state.
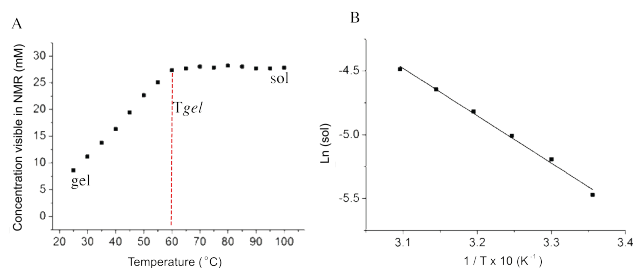
Journal Name

ARTICLE

Fig. 6 Determination of thermodynamic parameters. (A) Concentration of liquid-like phase free gelator as a function of temperature determined using fluorobenzene as an external standard in 2 % DMSO-d_6 + D$_2$O gel of **3-Fe**. (B) Vant Hoff´s treatment of VT NMR data, ln(solubility) against inverse of temperature.

A carefully designed NMR spectroscopy experiment can provide, not only the gel melting temperature and structural information about supramolecular interactions responsible of gelation, but also the concentration of the aggregated and non-aggregated components, enthalpy, entropy and free energy of gelation. It has been argued that the NMR resonances observed in a gel-phase at room temperature are largely resulting from the free molecules (mobile, non-aggregated components), whereas the aggregated components are NMR silent.[59,62] Experimental quantification is often achieved using a standard and monitoring the intensity of the observed gelator signal. In our experiment fluorobenzene was used as external standard in order to quantify the ratio between aggregated and non-aggregated fraction in the **3-Fe** gel upon increasing the temperature. The experiments were performed from 20 to 100°C with 5°C increment. When the concentration of the free molecules (in mM) was plotted against the temperature a steady increase until 60°C was observed (Fig. 6A). Above 60°C the concentration remained constant indicating that a gel-sol transition occurs at 60°C and all the components are disassembled. This temperature is slightly lower than the T$_{gel}$ value (T$_{gel}$ **3-Fe** = 69 °C) obtained by placing a sealed gel sample upside-down in a thermally controlled oil bath, increasing temperature and assigning the T$_{gel}$ as the temperature at which the gel starts to flow. In such experiments, done in an oil bath, the oil temperature might slightly differ from the temperature of the gel inside the test tube. Additionally, the conditions in which the gel undergoes transformation into a solution are different, therefore enabling small deviation within the T$_{gel}$ measurements through different methods. With increasing temperature the gel fibers disassemble due to thermal motion forming non-aggregated material and therefore sharper peaks. The process of disassembly can be considered as a solubilization process; therefore, the van´t Hoff treatment of the VT NMR data can be applied (See Fig. 6B and ESI).[17,63] The gelator molecules are considered to be soluble if they are observable by NMR and form insoluble aggregates if they are NMR silent. The data suitable for the van't Hoff treatment come from the measurements made well below T$_{gel}$ and above MGC in order to avoid initial steps of gelation. ΔH_{diss} and ΔS_{diss} are assumed to be temperature independent. For an ideal solution, the solubility (sol) at a

certain temperature can be fitted to van't Hoff equation (Eq. 1).

$$ln(Sol) = (-\Delta H_{diss}/RT_{eq}) + (\Delta S_{diss}/R) \qquad (1)$$

where ΔH_{diss} and ΔS_{diss} are enthalpy and entropy of dissolution, respectively. The T$_{eq}$ is the equilibrium temperature and R is the gas constant. The gelation process (which is the opposite of the dissolution process) is enthalpically favourable (ΔH_{diss} = 31(1) kJ mol^{-1}) and entropically disfavourable (ΔS_{diss}= 58(4) J mol^{-1} K^{-1}) as expected for an assembly of ordered fibers through hydrogen bonding and F···F interactions.[55] The value of the free energy is ΔG_{diss} = 13(2) kJ mol^{-1}. Moreover, a parallel van't Hoff study was performed by monitoring signal intensity of the gelator using VT ^{19}F NMR. The thermodynamical values obtained by applying van't Hoff treatment to VT ^{19}F NMR (ΔH_{diss} = 29(1) kJ mol^{-1}, ΔS_{diss} = 51(4) J mol^{-1} K^{-1} and ΔG_{diss} = 13(2) kJ mol^{-1}) are in a good agreement with the values obtained by VT ^{1}H NMR (See ESI). To the best of our knowledge, this is the first example where thermodynamic parameters of the sol-gel transition are obtained through VT ^{19}F NMR spectroscopy.

Rheological properties

In order to understand the mechanical properties and response to mechanical stimuli rheological measurements for aggregates of **3** and gels **3-Fe**, **3-Co** and **3-Ni** were carried out (Fig. 7). First, the sol-gel transition was investigated by using oscillatory time sweep experiment with 2 % gels from 20 min to 2 h. The time sweep experiments were performed within the viscoelastic regime (10 % strain) with 6.2 rad/s under controlled temperature (Fig. 7A). This experiment allows the gelation kinetics as there will be a rapid change in the storage (G') and loss modulus (G'') upon gel formation. On the other hand, it also provides information related to the time required to form a stable gel. The elastic modulus G´ for free ligand **3** was found to be 0.2 kPa which is an order of magnitude lower than that of the metallogels. Among metallogels the gel formation follows the order Fe>Co~Ni with elastic moduli **3-Ni**(1.6 kPa)>**3-Co**(1.4 kPa)>**3-Fe** (0.7 kPa) (Fig. 7A). The frequency sweep experiments showed that G´ of the gels is higher than G´´, confirming that the materials under study are viscoelastic solids (Fig. 7B). The gel-sol transition was followed using temperature sweep rheological experiment (Fig. 7C). Temperature ramps from 20 to 90 °C were performed with a 5 °C/min heating rate. Unlike many supramolecular gels, which show rapid changes in their elastic moduli upon gel-sol transition, the gels here showed some unique properties: they manifested two-step melting behaviour, where the elastic moduli of gels decreased rapidly by two orders of magnitude at around 45°C, 35°C and 55°C for **3-Fe, 3-Co** and **3-Ni** respectively (Fig. 7C). Further heating resulted in plateaus for 5 - 10°C before complete melting. This can be ascribed to the structural re-organization of the gel network and the role of several weak interactions responsible of gelation as shown by the VT NMR studies. The initial response can be attributed to
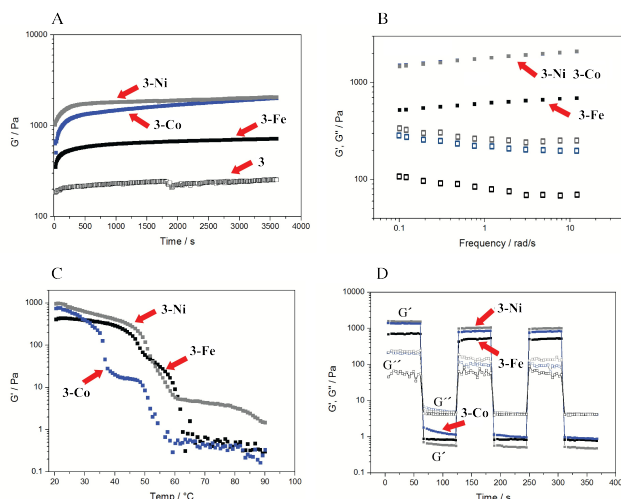
ARTICLE   Journal Name

Fig. 7 Rheological properties of 2 % DMSO/H$_2$O gels derived from gelators. (A) Time sweep experiments. (B) Frequency sweep. (C) Temperature sweep experiments. (D) Step strain experiments demonstrating fast self-healing.

the weakening of the F···F interactions, followed by a disruption of the H-bonding network. Then the step-strain experiment was performed in order to investigate the gel-sol transition and self-healing understood as the gel strength recovery, under several cycles. For the step strain experiments controlled strains of 0.1 % and 150 % were cycled for 60 s, respectively. The gels showed rapid response to increased strain by turning into viscoelastic liquids indicated by the rapid decrease in G´ by three orders of magnitude and well below that of G´´ (Fig. 7D). The application of increased strain also appears to break the structure further during the 60 s experiment as shown by gradually decreasing elastic moduli values. Upon switching to lower strain the gels recover most of their original mechanical strength almost instantly *i.e.* rapid self-healing. Additionally, the process can be repeated as shown in Figure 7D. However, slightly lower elastic moduli after first high-low strain cycle and gradual build-up is observed, therefore indicating that the structure build-up to equilibrium state would require longer periods of "rest" (low strain).

Conclusions

In conclusion, we have presented a simple terpyridine ligand decorated with a perfluoroalkyl chain that leads to metallosupramolecular gels in aqueous dimethyl sulfoxide. Our work demonstrates the importance of not only the fluorine - fluorine interactions but also the hydrogen bonding and the counter anion. Only chloride induces the gelation, therefore being anion specific with potential use in molecular recognition. Further, we showed that morphological, thermal and mechanical properties depend on the nature of the metal ion. Indeed, SEM and TEM images show clear differences on the size and morphology of the gel fibers. Additionally, **3-Fe** and **3-Ni** are thermally more stable than **3-Co**, meanwhile rheological experiments showed G´ follows the trend **3-Ni > 3-Co > 3-Fe**. Thermodynamic parameters of supramolecular gelation based on ^{1}H and; for the first time; by

^{19}F VT NMR resonances reveal that gelation is enthalpically favourable and entropically disfavourable. The excellent agreement between the results obtained by ^{1}H and ^{19}F VT NMR demonstrate the versatility of different spin active nuclei in determining thermodynamic parameters and could be further employed in supramolecular gels lacking hydrogen atoms. Metallogels undergo step-wise melting behaviour as suggested by ^{1}H NMR and supported by rheological measurements. More interestingly, metallogels exhibit self-healing properties under step-strain rheological experiment. Repeated cycles of high-low strain were applied to metallogels. A decrease of three orders of magnitude on the values of G´ turns into a fast strength recovery (self-healing) upon removing the strain. Our results suggest that incorporation of fluorine atoms induce metallogelation with novel thermal and mechanical properties.
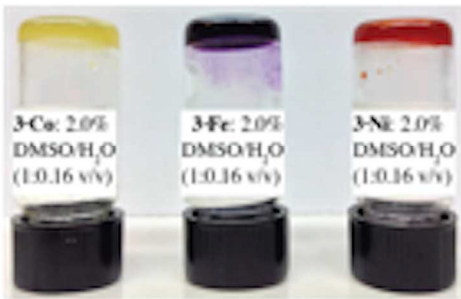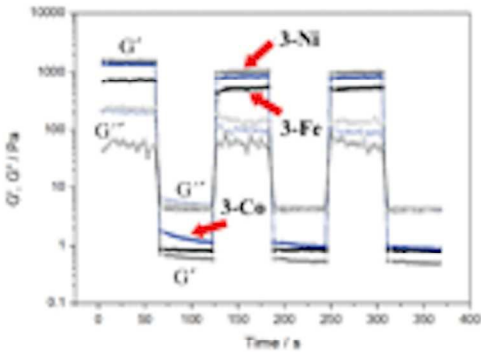
Acknowledgements

Notes and references

1   S. J. Dalgarno, N. P. Power and J. L. Atwood, *Coord. Chem. Rev.*, 2008, **252**, 825-841.
2   B. H. Northrop, Y.-R. Zheng, K.-W. Chi and P. J. Stang, *Acc. Chem. Res.*, 2009, **42**, 1554-1563.
3   B. J. Holliday and C. A. Mirkin, *Angew. Chem., Int. Ed.*, 2001, **40**, 2022-2043.
4   T. R. Cook, Y. R. Zheng and P. J. Stang, *Chem. Rev.*, 2013, **113**, 734-777.
5   J. Zhang and C.-Y. Su, *Coord. Chem. Rev.*, 2013, **257**, 1373-1408.
6   P. Mal, B. Breiner, K. Rissanen and J. R. Nitschke, *Science*, 2009, **324**, 1697-1699.
7   K. Suzuki, M. Tominaga, M. Kawano and M. Fujita, *Chem. Commun.*, 2009, 1638-1640.
8   M. Fujita, J. Yazaki and K. Ogura, *J. Am. Chem. Soc.*, 1990, **112**, 5645-5647 .
9   M. Fujita, Y. J. Kwon, S. Washizu and K. Ogura, *J. Am. Chem. Soc.*, 1994, **116**, 1151-1152.
10 B. Kersting, M. Meyer, R. E. Powers and K. N. Raymond, *J. Am. Chem. Soc.*, 1996, **118**, 7221-7222.
11 O. M. Yaghi, M. O'Keeffe, N. W. Ockwig, H. K. Chae, M. Eddaoudi and J. Kim, *Nature*, 2003, **423**, 705-714.
12 Q. Li, W. Zhang, O. Š. Miljanić, C.-H. Sue, Y.-L. Zhao, L. Liu, C. B. Knobler, J. F. Stoddart and O. M. Yaghi, *Science*, 2009, **325**, 855-859.
13 D. Fujita, K. Suzuki, S. Sato, M. Yagi-Utsumi, Y. Yamaguchi, N. Mizuno, T. Kumasaka, M. Takata, M. Noda, S. Uchiyama, K. Kato and M. Fujita, *Nat. Commun.*, 2012, **3**, 1093.
14 Y. Inokuma, S. Yoshioka and M. Fujita, *Ang. Chem. Int. Ed.*, 2010, **49**, 8912-8914.

15 M. Burnworth, L. Tang, J. R. Kumpfer, A. J. Duncan, F. L. Beyer, G. L. Fiore, S. J. Rowan and C. Weder, *Nature*, 2011, **472**, 334-337.

16 A. Aliprandi, M. Mauro, L. De Cola *Nat. Chem.*, 2016, **8**, 10-15.

17 A. R. Hirst, B. Escuder, J. F. Miravet and D. K. Smith, *Angew. Chem. Int. Ed.*, 2008, **47**, 8002-8018.

18 M. Maity and U. Maitra, *J. Mater. Chem. A*, 2014, **2**, 18952-18958.

19 P. Terech and R. G. Weiss, *Chem. Rev.*, 1997, **97**, 3133-3160.

20 L. A. Estroff and A. D. Hamilton, *Chem. Rev.*, 2004, **104**, 1201-1218.

21 T. Muraoka, H. Cui and S. I. Stupp, *J. Am. Chem. Soc.*, 2008, **130**, 2946-2947.

22 S. Grassi, E. Carretti, L. Dei, C. W. Branham, B. Kahr and R. G. Weiss, *New J. Chem.*, 2011, **35**, 445-452.

23 H. Svobodová, V. Noponen, E. Kolehmainen and E. Sievänen, *RSC Adv.*, 2012, **2**, 4985-5007.

24 A. E. Hooper, S. R. Kennedy, C. D. Jones and J. W. Steed, *Chem. Commun.*, 2016, **52**, 198-201.

25 G. Mieden-Gundert, L. Klein, M. Fischer, F. Vögtle, K. Heuzé, J.-L. Pozzo, M. Vallier and F. Fages, *Angew. Chem., Int. Ed.*, 2001, **40**, 3164-3166.

26 Y. C. Lin and R. G. Weiss, *Macromolecules*, 1987, **20**, 414-417.

27 P. Xue, H. Wu, X. Wang, T. He, R. Shen, F. Yue, J. Wang and Y. Zhang, *Sci. Rep.*, 2016, **6**, 25390.

28 J. van Esch, F. Schoonbeek, M. de Loos, H. Kooijman, A. L. Spek, R. M. Kellogg and B. L. Feringa, *Chem. Eur. J.*, 1999, **5**, 937-950.

29 M. D. Segarra-Maset, V. J. Nebot, J. F. Miravet and B. Escuder *Chem. Soc. Rev.*, 2013, **42**, 7086-7098.

30 H. Maeda, *Chem. Eur. J.*, 2008, **14**, 11274-11282, G. O. Lloyd and J. W. Steed, *Nat. Chem.*, 2009, **1**, 437-442.

31 Q. Lin, T. Lu, X. Zhu, T. Wei, H. Li and Y. Zhang *Chem. Sci.*, 2016, **7**, 5341-5346; Q. Lin, T. Lu, J. Lou, G. Wu, T. Wei and Y. Zhang, *Chem. Commun.*, 2015, **51**, 12224-12227.

32 W. Weng, J. B. Beck, A. M. Jamieson and S. J. Rowan, *J. Am. Chem. Soc.* 2006, **128**, 11663–11672; A. Y. Tam and V. W. Yam, *Chem. Soc. Rev.*, 2013, **42**, 1540-1567; N. Lanigan and X. Wang, *Chem. Commun.*, 2013, **49**, 8133-8144; M. M. Piepenbrock, G. O. Lloyd, N. Clarke and J. W. Steed, *Chem. Rev.*, 2010, **110**, 1960-2004.

33 R. Tatikonda, K. Bertula, Nonappa, S. Hietala, K. Rissanen and M. Haukka, *Dalton Trans.*, 2017, **46**, 2793-2802.

34 H. Bunzen, Nonappa, E. Kalenius, S. Hietala and E. Kolehmainen, *Chem. Eur. J.*, 2013, **19**, 12978-12981.

35 L. Sambri, F. Cucinotta, G. De Paoli, S. Stagni and L. De Cola, *New. J. Chem.* 2010, **34**, 2093-2096

36 B. N. Ghosh, S. Bhowmik, P. Mal and K. Rissanen, *Chem. Commun.*, 2014, **50**, 734-736.

37 L. Meazza, J. A. Foster, K. Fucke, P. Metrangolo, G. Resnati and J. W. Steed, *Nat. Chem.*, 2013, **5**, 42-47.

38 A. Bertolani, L. Pirrie, L. Stefan, N. Houbenov, J. S. Haataja, L. Catalano, G. Terraneo, G. Giancane, L. Valli, R. Milani, O. Ikkala, G. Resnati and P. Metrangolo, *Nat. Commun.*, 2015, **6**, 7574.

39 E. Faggi, R. M. Sebastián and A. Vallribera, *Tetrahedron*, 2010, **66**, 5190-5195.

40 S. Maity, P. Das and M. Reches, *Sci. Rep.*, 2015, **5**, 16365.

41 S. Banerjee, V. M. Vidya, A. J. Savyasachi and U. Maitra, *J. Mater. Chem.*, 2011, **21**, 14693-14705.

42 H. Kumari, S. E. Armitage, S. R. Kline, K. K. Damodaran, S. R. Kennedy, J. L. Atwood and J. W. Steed, *Soft Matter*, 2015, **11**, 8471-8478.

43 R. Tatikonda, S. Bhowmik, K. Rissanen, M. Haukka and M. Cametti, *Dalton Trans.*, 2016, **45**, 12756-12762.

44 I. T. Horváth and J. Rábai, *Science*, 1994, **266**, 72-75.

45 H.-J. Böhm, D. Banner, S. Bendels, M. Kansy, B. Kuhn, K. Müller, U. Obst-Sander and M. Stahl, *ChemBioChem*, 2004, **5**, 637-643.

46 G. Gerebtzoff, X. Li-Blatter, H. Fischer, A. Frentzel and A. Seelig, *ChemBioChem*, 2004, **5**, 676-684.

47 R. J. Baker, P. E. Colavita, D. M. Murphy, J. A. Platts and J. D. Wallis, *J. Phys. Chem. A.*, 2012, **116**, 1435-1444.

48 H. Omoodion, B. Twamley, J. A. Platts and R. J. Baker, Crystal Growth & Design, 2015, **15**, 2835-2841.

49 E. Krieg, H. Weissman, E. Shimoni, A. Bar On Ustinov and B. Rybtchinski, *J. Am. Chem. Soc.*, 2014, **136**, 9443-9452.

50 B. Xu, L. Li, A. Yekta, Z. Masoumi, S. Kanagalingam, M. A. Winnik, K. Zhang, P. M. Macdonald and S. Menchen, *Langmuir*, 1997, **13**, 2447-2456.

51 Y. X. Zhang, A. H. Da, T. E. Hogen-Esch and G. B. Butler, *ACS Symposium Series*, 1991, **467**, 159-174.

52 C. Shi, Z. Huang, S. Kilic, J. Xu, R. M. Enick, E. J. Beckman, A. J. Carr, R. E. Melendez and A. D. Hamilton, *Science*, 1999, **286**, 1540-1543.

53 M. George, S. L. Snyder, P. Terech, C. J. Glinka and R. G. Weiss, *J. Am. Chem. Soc.*, 2003, **125**, 10275-10283.

54 T. Yoshida, T. Nakamura, Y. Morita and H. Okamoto, *Chem. Lett.*, 2015, **44**, 512-514.

55 B. Cao, Y. Kaneshige, Y. Matsue, Y. Morita and H. Okamoto, *New J. Chem.*, 2016, **40**, 4884-4887.

56 S. Strandman and X. X. Zhu, *Gels*, 2016, **2**, 16.

57 J. Wang and G. S. Hanan, *Synlett*, 2005, 1251-1254.

58 W. Liyanage, W. W. Brennessel and B. L. Nilsson, *Langmuir*, 2015, **31**, 9933-9942; A. D. Martin, J. P. Wojciechowski, M. M. Bhadbhade and P. Thordarson, *Langmuir*, 2016, **32**, 2245-2250; I. Ramos Sasselli, P. J. Halling, R. V. Ulijn, and T. Tuttle, *ACS Nano*, 2016, **10**, 2661-2668; D. Braga, S. d'Agostino, E. D'Amen and F. Grepioni, *Chem. Commun.*, 2011, **47**, 5154-5156; C. D. Jones, J. C. Tan and G. O. Lloyd, *Chem. Commun.*, 2012, **48**, 2110-2112; S. Samai, P. Ghosh and K. Biradha, *Chem. Commun.*, 2013, **49**, 4181-4183; J. Gao, S. Wu, T. J. Emge and M. A. Rogers, *CrystEngComm*, 2013, **15**, 4507-4515; C. Zhao, Y. Li, X. Wang, G. Chen, Q. Liu, J. Ma and Y. Dong, *Chem. Commun.*, 2015, **51**, 15906-15909; J. Schiller, J. V. Alegre-Requena, E. Marqués-López, R. P. Herrera, J. Casanovas, C. Alemán and D. Díaz Díaz, *Soft Matter*, 2016, **12**, 4361-4374; S. Saha, G. Das, J. Thote and R. Banerjee; *J. Am. Chem. Soc.*, 2014, **136**, 14845-14851; Y. Wang, W. Qi, R. Huang, X. Yang, M. Wang, R. Su and Z. He, *J. Am. Chem. Soc.*, 2015, **137**, 7869-7880; G. K. Veits, K. K. Carter, S. J. Cox and A. J. McNeil, *J. Am. Chem. Soc.*, 2016, **138**, 12228-12233; I. Kapoor, E. Schön, J. Bachl, D. Kühbeck, C. Cativiela, S. Saha, R. Banerjee, S. Roelens, J. J. Marrero-Tellado and D. Díaz Díaz, *Soft Matter*, 2012, 8, 3446-3456; E. C. Barker, A. D. Martin, C. J. Garvey, C. Y. Goh, F. Jones, M. Mocerino, B. W. Skelton, M. I. Ogden and T. Becker, *Soft Matter*, 2017, **13**, 1006-1011; A. Biswas, M. Dubey, S. Mukhopadhyay, A. Kumar and D. S. Pandey, *Soft Matter*, 2016, **12**, 2997-3003; A. Vidyasagar and K. M. Sureshan, *Angew. Chem., Int. Ed.*, 2015, 54, 12078-12082.

59 B. Escuder, M. Llusar and J. F. Miravet, *J. Org. Chem.*, 2006, **71**, 7747-7752.

60 Nonappa and E. Kolehmainen, *Soft Matter*, 2016, **12**, 6015-6026; Nonappa, M. Lahtinen, B. Behera, E. Kolehmainen and U. Maitra, *Soft Matter*, 2010, **6**, 1748-1757; Nonappa, D. Saman and E. Kolehmainen, *Magn. Reson. Chem.*, 2015, **53**, 256-260.

61 R. Wang, C. Wang, Y. Cao, Z. Zhu, C. Yang, J. Chen, F. Qing and W. Tan, *Chem. Sci.*, 2014, **5**, 4076-4081.

62 M. Wallace, J. A. Iggo and D. J. Adams, *Soft Matter*, 2015, **11**, 7739-7747.

63 W. Edwards and D. K. Smith, *J. Am. Chem. Soc.*, 2013, **135**, 5911-5920.

Metal complexes from a perfluoroalkylamide terpyridine self-assemble into anion selective gels, which manifest self-healing and thermal rearrangement in aqueous-dimethyl sulfoxide.

TOC figure